The Journal of Neuroscience, December 1, 1997, 17(23):9035–9047

Mutation Causing Autosomal Dominant Nocturnal Frontal Lobe Epilepsy Alters Ca^{2+} Permeability, Conductance, and Gating of Human $\alpha4\beta2$ Nicotinic Acetylcholine Receptors

Alexander Kuryatov, Volodymyr Gerzanich, Mark Nelson, Felix Olale, and Jon Lindstrom

Department of Neuroscience, Medical School, University of Pennsylvania, Philadelphia, Pennsylvania 19104-6074

A mutation (S247F) in the channel-lining domain (M2) of the $\alpha4$ nicotinic acetylcholine receptor (AChR) subunit has previously been linked genetically to autosomal dominant nocturnal frontal lobe epilepsy (ADNFLE).

To better understand the functional significance of this mutation, we characterized the properties of mutant and wild-type human $\alpha4\beta2$ AChRs expressed in *Xenopus* oocytes. Both had similar expression levels and EC_{50} values for ACh and nicotine. Substantial use-dependent functional upregulation was found for mutant $\alpha4\beta2$ AChRs, but not for wild type. Mutant AChR responses showed faster desensitization, slower recovery from desensitization, less inward rectification, and virtually no Ca^{2+} permeability as compared with wild-type $\alpha4\beta2$ AChRs. Addition of the $\alpha5$ subunit restored Ca^{2+} permeability to the mutant $\alpha4\beta2\alpha5$ AChRs. At -80 mV, wild-type $\alpha4\beta2$ AChR single channel currents exhibited two conductances, each with two mean open times ($\gamma_1 = 17$ pS, $\tau_1 = 3.7$ msec, and $\tau_2 = 23.4$ msec; $\gamma_2 = 28$ pS, $\tau_1 = 1.9$ msec, and $\tau_2 = 8.1$ msec). In contrast, mutant AChRs exhibited only one conductance of 11 pS, with $\tau_1 = 1.9$ msec and $\tau_2 = 4.1$ msec.

The net effect of the mutation is to reduce AChR function. This could result in the hyperexcitability characteristic of epilepsy if the mutant AChRs were part of an inhibitory circuit, e.g., presynaptically regulating the release of GABA. In the minority of AChRs containing the $\alpha5$ subunit, the overall functionality of these AChRs could be maintained despite the mutation in the $\alpha4$ subunit.

Key words: autosomal dominant nocturnal frontal lobe epilepsy; nicotinic acetylcholine receptors; calcium permeability; desensitization; epilepsy; single channel

Autosomal dominant nocturnal frontal lobe epilepsy (ADNFLE) is a recently recognized form of epilepsy in which brief partial seizures occur during light sleep and often are misdiagnosed as nightmares (Scheffer et al., 1994). ADNFLE is the first inherited epilepsy in which a specific mutation has been identified (Phillips et al., 1995; Scheffer et al., 1994, 1995; Steinlein et al., 1995). ADNFLE patients exhibit a missense mutation in $\alpha4$ subunits of neuronal nicotinic acetylcholine receptors (AChRs), causing serine to be replaced with phenylalanine at position 247 (Steinlein et al., 1995). This replaces a highly conserved small hydrophilic amino acid with a large hydrophobic amino acid at a region of the M2 transmembrane domain thought to line the AChR cation channel near the channel gate at the cytoplasmic surface (Akabas et al., 1994). Recently, a second mutation involving insertion of a leucine near the extracellular end of M2 also has been found to cause ADNFLE (Steinlein et al., 1997).

$\alpha4$ subunits form neuronal AChRs that have the subunit composition $(\alpha4)_2(\beta2)_3$ (Anand et al., 1991; Cooper et al., 1991). In mammalian brains, $\alpha4$ AChRs comprise the major AChR subtype, with high affinity for nicotine (Whiting and Lindstrom, 1988). A small fraction of these AChRs may have $\alpha5$ subunits associated with them (Ramirez-Latorre et al., 1996). $\alpha4$ AChRs are expressed in many brain regions (Wada et al., 1989; Lindstrom et al., 1995), yet the functional roles of $\alpha4$ AChRs are not clearly defined. Many neuronal AChRs are thought to be located presynaptically where they can modulate neurotransmitter release (Role and Berg, 1996; Wonnacott, 1997). Post- and perisynaptic roles for AChRs in peripheral ganglionic synaptic transmission are well known; however, it has been difficult to demonstrate similar involvement of AChRs in central synaptic transmission except at brain stem vagal motor neurons (Zhang et al., 1993). Nicotine has been reported to improve concentration, alertness, and memory, and it is supposed that these effects would be mediated via $\alpha4\beta2$ AChRs and other subtypes of neuronal AChRs (Riedel and Jolles, 1996; Vidal and Changeux, 1996).

Recent studies on recombinant $\alpha4\beta2$ AChRs containing the $\alpha4$ subunit S247F mutation showed that these AChRs exhibit significantly faster desensitization and slower recovery from the desensitized state as compared with wild type (Weiland et al., 1996). Thus, it was proposed that this reduction in $\alpha4\beta2$ activity might disturb the balance between inhibitory and excitatory synaptic transmission, thereby lowering the seizure threshold.

Serine 247 of $\alpha4$ subunits is thought to contribute to the hydrophilic lining of the cation-selective channel through the center of the AChR molecule. In all AChR subunits there are small hydrophilic amino acids (either serine or threonine) at this position, so changing this residue to a larger hydrophobic phenylalanine might be expected to alter channel conductance. It has been shown that this mutation in muscle $\alpha1$ AChR subunits decreases channel conductance by 25% but increases sensitivity to ACh by eightfold (Forman et al., 1996). Changes in potency of agonists because of mutations in the AChR channel lining are

Received July 7, 1997; revised Sept. 17, 1997; accepted Sept. 18, 1997.

This work was supported by grants to J.L. from the National Institutes of Health (NS11323), the Smokeless Tobacco Research Council, Incorporated, and the Muscular Dystrophy Association. M.N. was supported by a National Research Service Award fellowship.

A.K., V.G., and M.N. contributed equally to this work.

Correspondence should be addressed to Dr. Jon Lindstrom, 217 Stemmler Hall, Department of Neuroscience, Medical School of the University of Pennsylvania, Philadelphia, PA 19104-6074.

thought to result from changes in channel gating (Bertrand et al., 1993; Filatov and White, 1995).

To understand the pathological mechanisms resulting from the α4 S247F mutation, we compared in detail the expression, kinetics, pharmacology, and channel properties of mutant and wild-type α4β2 AChRs. Additionally, we investigated the influence of the α5 AChR subunit, which can associate with α4 and β2 subunits to form functional AChRs (Ramirez-Latorre et al., 1996).

MATERIALS AND METHODS

Cloning and mutation of the human α4 AChR subunit. The cDNA encoding the human neuronal AChR α4 subunit was obtained by PCR amplification of cDNA synthesized from human brain poly(A^+) RNA (Clontech, Palo Alto, CA) with StrataScript RNase H^- Reverse Transcriptase (Stratagene, La Jolla, CA), using two sets of primers (forward GCCAGCAGCCATGTGGAG, reverse GCCATCTTATGCATGGACTCGATG; forward TGGGTACGCAGGGTCTTC, reverse AGCAGGCTCCCGGTCCCTTCCTAG). For subsequent recloning into a vector, these PCR products were digested enzymatically with *Bsa*I, *Nsi*I, and *Nsi*I endonucleases. The 5′ end of this subunit was amplified from 5′-RACE-Ready cDNA (Clontech), using the Anchor Primer supplied with the kit (CTGGTTCGGCCCACCTCTGAAGGTTCCAGAATCGATAG) and a specific 5′ reverse primer (GCCACGGGTCGGGACCAC). The 5′ end PCR fragment was digested with *Cla*I and *Bsa*I restriction enzymes. All PCR fragments were purified by agarose gel electrophoresis with the Geneclean II kit (BIO 101, Vista, CA). The PCR products were ligated together via *Bsa*I and *Nsi*I sites and cloned into the *Cla*I and *Eco*RV blunt end sites of the pBluescript II SK(−) phagemid. To add a poly(A^+) tail, we recloned this construct into *Sal*I and *Bam*HI sites of a modified pSP64 poly(A^+) plasmid, where an *Ase*I site can be used for linearization instead of *Eco*RI. The construct was sequenced according to the Sanger method (Sequenase Version 2.0 DNA Sequencing Kit; United States Biochemical, Cleveland, OH) to verify the published sequence of the human α4 AChR subunit (Gopalakrishnan et al., 1996).

For introduction of the mutation S247 to F247 into the human α4 subunit, a 316 bp fragment was amplified by PCR, using the primer AGATCACGCTGTGCATCTTCGTGCTG (in which the nucleotide responsible for this mutation is underlined) and the primer sequence GCCATCTTATGCATGGACTCGATG from the cloned subunit. This fragment was recloned into the α4 subunit by using the *Dra*III and *Nsi*I restriction sites. The fragment was sequenced according to the Sanger method (Sequenase Version 2.0 DNA Sequencing Kit, United States Biochemical) to verify that only the desired mutation was present.

cDNAs encoding the human α4 and S247F α4 subunits were cloned into a modified pSP64 poly(A^+) (Promega, Madison, WI) expression vector with a unique *Eco*RI site and digested; sticky ends were filled in with Klenow enzyme (Boehringer Mannheim, Indianapolis, IN) and religated with T4 DNA polymerase (New England Biolabs, Beverly, MA). α5 and β2 were cloned in the pSP64 poly(A^+) vector, using standard DNA cloning procedures (Melton et al., 1984). cRNA was synthesized *in vitro* with the Megascript kit (Ambion, Austin, TX).

The oocytes were removed surgically from *Xenopus laevis* (Xenopus I, Ann Arbor, MI) and placed in oocyte physiological saline (ND-96) containing (in mM) 96 NaCl, 2 KCl, 1.8 $CaCl_2$, 1 $MgCl_2$, and 10 HEPES, pH 7.5, to which 50 U/ml of penicillin and 50 μg/ml of streptomycin were added. Oocytes were dispersed in this buffer minus Ca^{2+} containing 2 mg/ml collagenase A (Sigma, St. Louis, MO) for 2 hr.

Stage V–VI oocytes were selected and injected with combinations of α4β2, α4β2α5, α4S247Fβ2, and α4S247β2α5 subunit cRNAs (equal amounts of 5–12 ng of each subunit in a total volume of 55 nl). After injections, oocytes were maintained semisterile at 18°C in Liebovitz L-15 medium (Life Technologies, Grand Island, NY) diluted by one-half in 10 mM HEPES buffer, pH 7.5.

Electrophysiology and perfusion solutions; whole-cell recordings. Currents were measured with a standard two-microelectrode voltage-clamp amplifier (Oocyte Clamp OC-725; Warner Instrument, Hamden, CT) as previously described (Gerzanich et al., 1994). All recordings were digitized at 200 Hz with MacLab software and hardware (AD Instruments, Castle Hill, Australia) and stored on an Apple Macintosh IIcx computer (Cupertino, CA). Data were analyzed by using KALEIDAGRAPH (Synergy Software, Reading, PA).

The recording chamber was perfused at a flow rate of 10 ml/min with ND-96 solution. All perfusion solutions contained 0.5 μM atropine. Agonists were applied, using a set of eight glass tubes as previously described (Gerzanich et al., 1994). For experiments measuring the effect of extracellular Ca^{2+} on the reversal potentials, intracellular electrodes were filled with 2.5 M potassium aspartate. To prevent activation of the endogenous Ca^{2+}-dependent Cl^- channels, we used Cl^--free solutions for oocyte preincubation (6–12 hr) and for the perfusion during recordings (Francis and Papke, 1996). "Normal" Ca^{2+} solution included (in mM) 90 $NaMeSO_3$, 2.5 KOH, 10 HEPES, and 1.8 $Ca(OH)_2$. Additionally, 48 mM dextrose was supplemented in the normal solution to yield osmolarity equal to the "high" Ca^{2+} solution, which contained 18 mM $Ca(OH)_2$ and the same concentration of the other ions as "normal" Ca^{2+} solution. Both solutions were buffered with methanesulfonic acid to pH 7.3. Reversal potentials of the currents were determined either by 6 sec agonist applications at different holding potentials or by 2 sec ramps of the holding potential from −50 to +50 mV during agonist application after the current reached a steady state. Both protocols gave similar estimates for the reversal potential. Control ramp currents obtained before agonist applications were subtracted from the ramp currents during AChR activation. In one set of experiments current carried by Ca^{2+} ions only was measured by using solutions containing only 1.8 mM $Ca(OH)_2$ buffered to pH 7.3 by HEPES. Dextrose (at 200 mM) was added to the solutions to preserve osmolarity.

Single channel recordings. *Xenopus* oocytes were manually stripped of the vitelline membrane after osmotic shrinking with a 200 mM potassium aspartate solution. Outside-out configuration patches were formed from stripped oocytes expressing recombinant AChRs 5–10 d after cRNA injections. Single channel currents were activated by the application of ACh flowing continuously from one barrel of a two-barrel fused glass capillary tubing that was attached to as many as 10 different reservoirs among which selections were made by two six-way valves (Rheodyne, Cotati, CA) in series. Before application of agonist, the patch was isolated in a continuously flowing control solution from the other barrel of the fused glass tubing. The change to the agonist-containing solution was achieved by manually repositioning the perfusion tubing in a lateral direction. The recording solutions were an ND-96 bath solution and a pipette solution consisting of (in mM) 80 CsF, 20 CsCl, 10 Cs-EGTA, 10 HEPES, and 3 MgATP, pH-adjusted to 7.2 with CsOH. Electrodes were formed from borosilicate glass tubing and had resistances of 7–15 mΩ. Recordings were obtained with an Axopatch 1-D amplifier (Axon Instruments, Foster City, CA) and sampled with an VR-10A digital data recorder (Instrutech, Great Neck, NY) onto video medium (VHS model VC-A206C, Sharp, Osaka, Japan) for later analysis. Signals were sampled off-line at 10 kHz (Axotape 2.0, Axon Instruments) and filtered at 2 kHz (Model 902; eight-pole Bessel, −3 dB; Frequency Devices, Haverhill, MA) for analysis, except for some mutant α4β2 AChR recordings that were filtered at 1.5 kHz because of the low signal-to-noise ratios. All single channel analysis and fitting were performed with pClamp 6.0.3 (Axon Instruments). Events list files were formed by visual inspection of the data and manually accepting or rejecting putative events while ignoring events <0.2 or 0.3 msec in duration (depending on filter bandwidth). Then the data in the events list files were log-binned into histograms, using seven to eight bins per decade, and fit with single- or double-exponential functions, using maximum likelihood optimization of a Simplex algorithm (Sigworth and Sine, 1987). The number of components in the "best" fit were evaluated visually and also by comparing the likelihood ratios of the fits. For figures, histograms with fits were exported to Origin (Microcal Software, Northampton, MA). Representative single channel traces were constructed by opening data files in Axograph 3.55 (Axon Instruments) for the Power Macintosh 7100 (Apple Computer) and exporting data segments to Canvas 5.0 (Daneba Software, Miami, FL).

Monoclonal antibodies (mAbs) used, oocyte surface AChRs binding, and solid phase radioimmunoassay (RIA). Immulon 4 (Dynatech, Chantilly, VA) microtiter wells were coated with mAbs 290, 299, or 210 (Wang et al., 1996) as described previously (Anand et al., 1993). Oocytes were homogenized by repetitive pipetting in buffer [containing (in mM) 50 Na_2HPO_4–NaH_2PO_4, pH 7.5, 50 NaCl, 5 EDTA, 5 EGTA, 5 benzamidine, 15 iodoacetamide, and 2 phenylmethylsulfonyl fluoride]. The membrane fractions were collected by centrifugation (15 min at 15,000 × *g*). AChRs were solubilized by incubating the membrane fractions in the same buffer containing 2% Triton X-100 at 4°C for 1 hr. Nonsolubilized fractions were removed by centrifugation for 15 min at 15,000 × *g*. Solubilized AChRs from oocytes were used directly for all assays. mAb-

coated microtiter wells were incubated with Triton-solubilized AChRs and 5 nM ^{3}H-epibatidine (DuPont NEN, Boston, MA) at 4°C for 16 hr. Then the wells were washed three times with ice-cold PBS and 0.05% Tween-20 buffer; the amount of radioactivity bound was determined by liquid scintillation counting. The nonspecific binding was determined by processing the RIAs with extracts of noninjected oocytes.

Surface binding. Surface expression was determined by incubating oocytes in ND-96 solution containing normal adult bovine serum and 10 nM ^{125}I-mAb ($0.5–2 \times 10^{18}$ cpm/mol for 1 hr at 25°C) with stirring, followed by three washes with ND-96 to remove nonspecific binding. Nonspecific binding was determined by incubating noninjected oocytes under the same conditions.

RESULTS

Expression and time course of the responses of wild-type and S247F human α4β2 AChRs

Levels of surface expression and ACh-induced currents of α4β2 and α4β2α5 AChRs incorporating wild-type and mutated α4 subunits were determined 3–6 d after cytoplasmic injection of the subunit cRNAs into *Xenopus* oocytes. Surface binding of ^{125}I-mAb290 specific for β2 subunits indicated high efficiency of expression, with levels of binding ranging from 1 to 7 fmol/oocyte. Maximum ACh-induced currents were correspondingly large, reaching 20 μA at −50 mV. Mutant α4β2 AChRs, both without and with α5 subunit incorporated, showed equivalent levels of surface expression similar to wild-type α4β2 AChRs (Fig. 1). When α4, β2, and α5 cRNAs were injected in a 1:1:1 ratio, surface levels of ^{125}I-mAb290 binding to β2 subunits were lower by 15–30% (Fig. 1) as compared with α4β2 AChRs. Functionality of the expressed AChRs was tested by measuring net charge carried during responses induced by a saturating concentration of ACh (100 μM) before surface labeling with ^{125}I-mAb210 (Fig. 1). Mutant α4β2 AChRs carried 60% less charge per AChR than did wild type. Native α4β2α5 AChRs carried 25% less charge per AChR than did native α4β2 AChRs, and mutant α4β2α5 AChRs carried 30% less charge than did this wild-type combination of subunits.

α5 subunits assembled very efficiently with both wild-type and mutant α4β2 AChRs. After coinjection of the cRNAs for α5, β2, and α4 wild-type or mutant subunits in a 1:1:1 ratio, AChRs were immunoisolated, using mAbs specific for each subunit; the amount of AChR isolated by each antibody was determined by binding of ^{3}H-epibatidine (Fig. 1). Each of the mAbs tested isolated the same amount of AChR, suggesting that all three types of subunits were incorporated in virtually all AChRs. mAb210 binds to the main immunogenic region epitope expressed on the extracellular surface of α1, α3, and α5 subunits (Wang et al., 1996) but does not bind to α4 subunits (data not shown). mAb290 and mAb299 (Whiting and Lindstrom, 1988) bind to the extracellular surfaces of β2 and α4 subunits, respectively, and previously have been used to quantitate α4β2 AChRs expressed in oocytes (Peng et al., 1994).

Mutant α4β2 AChRs exhibited a peculiar facilitation response to agonists. In oocytes expressing mutant α4β2 AChRs, responses induced by the initial agonist application augmented with consecutive applications, reaching a plateau after five to six activations (Fig. 2). Thus, the first application of ACh induced a rather small current, which increased more than threefold, on average, before plateauing at the new level. The time course of the responses did not change significantly during this process. When the same oocytes were tested 24 hr later, they exhibited no additional increase of response with consecutive applications of agonist. The response increase was observed only for naive oocytes not previously exposed to agonist. This phenomenon of initial activation-dependent functional upregulation was not observed in oocytes expressing wild-type α4β2 AChRs, in which the amplitude of the response remained virtually the same during consecutive applications of the agonist (Fig. 2). These results suggest that exposure to agonists can cause a long-lived or permanent change in the conformation of mutant α4β2 AChRs to a more activatable conformation. To test whether this use-dependent upregulation of function might be caused by displacing from the mutant channel antibiotics or other components of the L-15 medium in which injected oocytes were incubated routinely, we incubated oocytes in ND-96 solution instead. After incubation of injected oocytes in ND-96, mutant α4β2 AChRs still exhibited use-dependent upregulation. Thus, this phenomenon cannot be attributable to displacement from mutant channels of antibiotics or other organic compounds in L-15 medium, but it cannot be excluded that an inorganic ion was displaced from mutant channels.

To exclude the possible influence of the endogenous Ca^{2+}-dependent Cl^{-} current in *Xenopus* oocytes, which can distort the time course of the responses mediated via neuronal nicotinic AChRs (Leonard and Kelso, 1990; Vernino et al., 1992; Gerzanich et al., 1994), we recorded responses in Cl^{-}-free media. Moreover, oocytes were preincubated in the Cl^{-}-free media for 4–16 hr before recordings, and recordings were performed with electrodes filled with Cl^{-}-free solution (potassium aspartate). Concentration of Ca^{2+} ions in the extracellular solution was maintained at 1.8 mM to correspond to the Ca^{2+} concentration in normal recording conditions. These conditions were preferable to those applied in the previous study of S247F α4β2 AChRs (Weiland et al., 1996), where, to prevent activation of Ca^{2+}-dependent Cl^{-} currents, recordings were performed in media in which Mg^{2+} ions were substituted for Ca^{2+} ions. Extracellular Ca^{2+} is known to modulate such properties of nicotinic AChRs as conductance, open probability, and desensitization (Vernino et al., 1992). Furthermore, increase of extracellular Mg^{2+} potentially could cause channel block that could be altered by the S247F mutation.

The S247F mutation in α4 subunits caused changes in the rates of desensitization of both α4β2 and α4β2α5 AChRs. Normalized current traces obtained from oocytes expressing mutant and wild-type α4β2 and α4β2α5 AChRs are superimposed for comparison in Figure 2. Each trace shown represents the average of normalized currents from 15 to 22 oocytes induced by a saturating concentration of ACh. Wild-type α4β2 AChRs did not show significant desensitization over 30 sec. In contrast, current through the mutant AChRs fell rapidly by ~50% and then continued to decay slowly in the presence of ACh. The time constant for the initial fast component of the desensitization was 1.8 sec, and the time constant for the secondary component was 45 sec. When the α5 subunit was coexpressed with wild-type α4β2 AChRs, responses exhibited notable desensitization as compared with α4β2 AChRs without α5 (Fig. 2, *bottom right*). The currents decayed with a time constant of 6.4 sec to a plateau level of ~65%. For mutant α4β2α5 AChRs, the initial component of desensitization was somewhat faster as compared with the wild type, with a time constant of 4.5 sec. The current decay continued in the presence of ACh after the initial peak with a time constant of ~40 sec, resembling the slow component of desensitization of mutant α4β2 AChRs (Fig. 2, *bottom*). Recovery from desensitization of mutant α4β2 and α4β2α5 AChRs also was much slower as compared with wild-type α4β2α5 AChRs (data not shown).

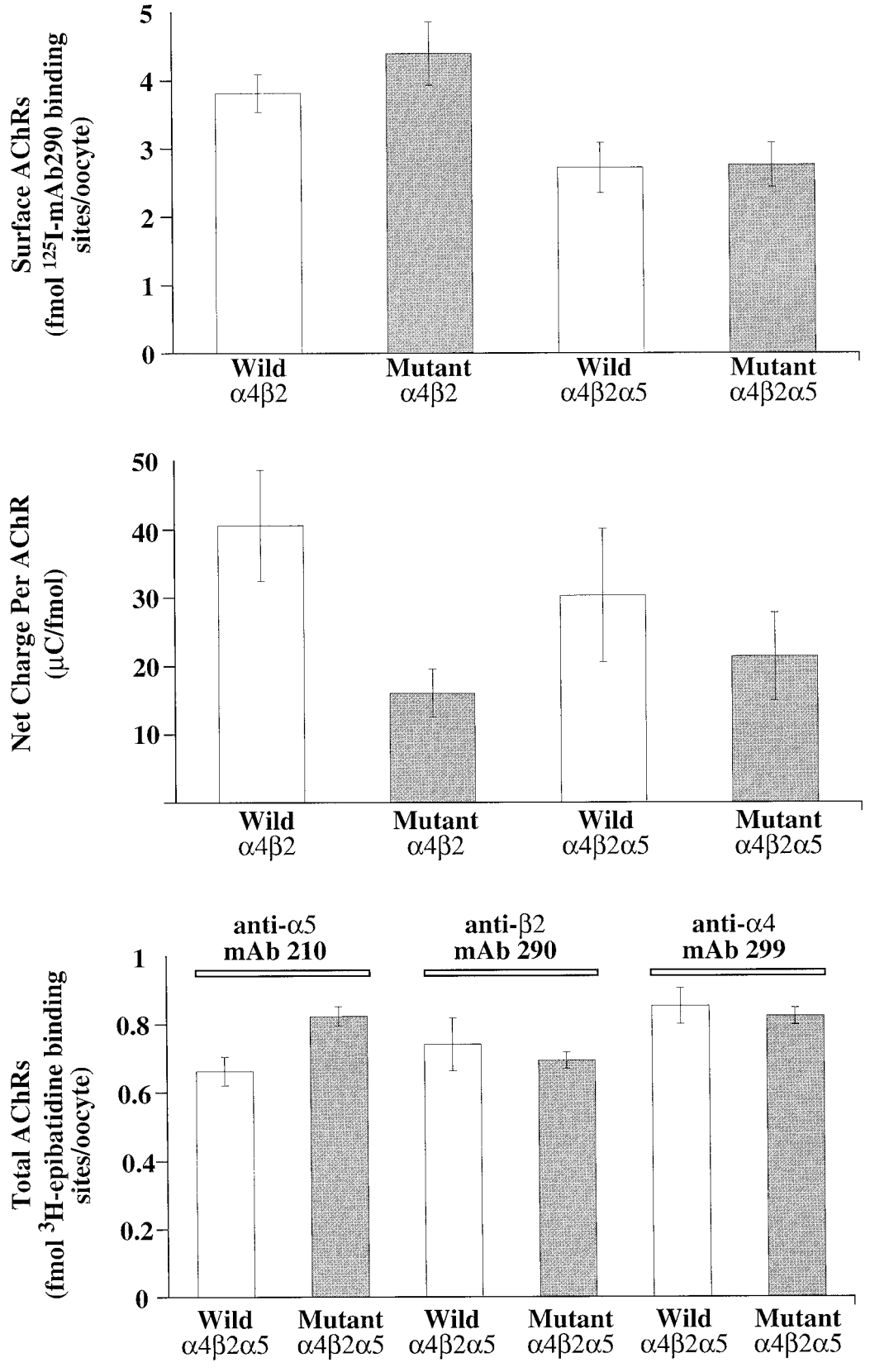

Figure 1. Expression levels are not impaired by the S247F mutation. *Top*, Comparison of surface expression of AChRs per oocyte detected by binding of ^{125}I-mAb290 to β2 subunits on the surface of intact oocytes. *Middle,* Average amounts of net charge carried per femtomole of surface AChRs. Inward currents induced by an initial 30 sec exposure to 100 μM ACh at −30 mV in Cl^--free medium were integrated. *Bottom,* Total AChRs immunoisolated from detergent extracts of oocytes, using mAbs specific for either α3 and α5 subunits (mAb210), β2 subunits (mAb290), or α4 subunits (mAb299). Data were obtained from 7 to 10 oocytes for each measurement. The mean value and SE are shown.

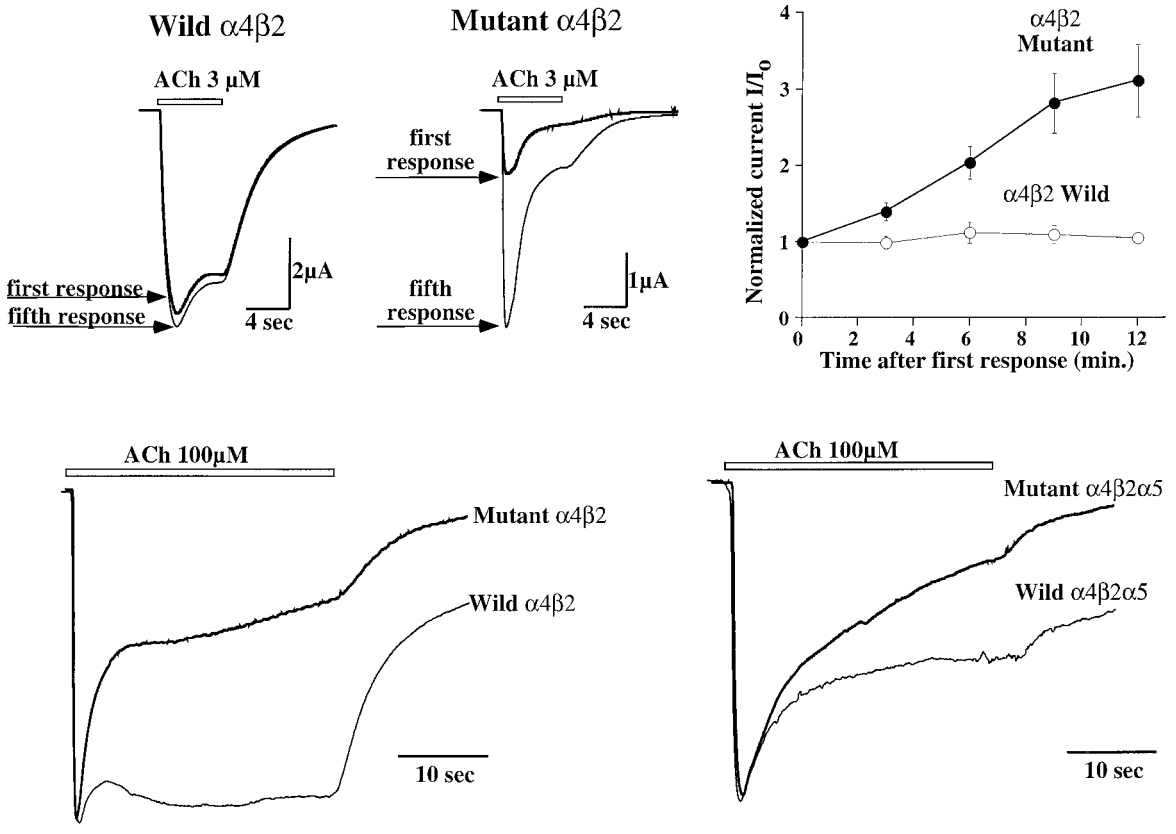

Figure 2. Functional differences between wild-type and mutant α4β2 AChRs. *Top*, Use-dependent functional upregulation of the responses mediated by mutant α4β2 AChRs. *Left*, Currents induced by the first and fifth application of 3 μM ACh are shown for oocytes expressing wild-type and mutant α4β2 AChRs. Oocytes that did not have previous exposure to the agonists were held at −50 mV. ACh was applied at 2 min intervals. *Right,* Plot of the response peak amplitude on the initial five consecutive applications of 3 μM ACh on the oocytes expressing wild-type (*open circles*) or mutant α4β2 AChRs (*filled circles*). Currents were normalized to the peak amplitude of the first response. *Bottom*, S247F mutation causes significant changes in the desensitization of the α4β2 and α4β2α5 AChRs. *Left,* Comparison of the time course of the superimposed normalized averaged currents mediated by the wild-type (*thin trace*) and mutant (*thick trace*) α4β2 AChRs. *Right,* Comparison of time course for the wild-type and mutant α4β2α5 AChRs. Averaged currents were obtained from 15 to 22 oocytes by normalizing to the same current amplitude. Oocytes were held at −50 mV. Both perfusion and agonist solution contained no Cl^- ions to prevent contamination with endogenous Ca^{2+}-dependent Cl^- current. Oocytes were preincubated in Cl^--free media for 4–16 hr.

Comparison of some pharmacological properties of wild-type and S247F α4β2 AChRs

Wild-type and mutant α4β2 AChRs showed subtle differences in sensitivity to ACh and nicotine (Fig. 3, *top*). ACh activated wild-type AChRs with an EC_{50} of 2.2 ± 0.1 μM [Hill coefficient of the concentration/response curve (*n*H) was 2.1]. The ACh concentration/response curve for mutant AChRs had a Hill coefficient of 0.9 and an EC_{50} value of 11.6 ± 1.2 μM. Similarly, the mutant AChRs had lower sensitivity to nicotine (EC_{50} = 1.8 ± 0.6 μM) as compared with wild-type α4β2 AChRs (EC_{50} = 0.3 ± 0.04 μM), although Hill coefficients for both were >1 (1.8 and 1.4, respectively). The efficacy of nicotine for both wild-type and mutant α4β2 AChRs was slightly lower (~90%) as compared with ACh (Fig. 3, *top*).

Inhibition by a competitive ACh binding site antagonist and by quinine was equivalent for both wild-type and mutant α4β2 AChRs, whereas inhibition by the noncompetitive ion channel blocker amantadine was less potent on mutant α4β2 AChRs. Both wild-type and mutant α4β2 AChRs were inhibited effectively and reversibly by the competitive antagonist dihydro-β-erythroidine (DHβE) (Harvey et al., 1996) (Fig. 3, *left*). Additionally, amantadine (Matsubayashi et al., 1997) and quinine blocked both wild-type and mutant AChRs, although at concentrations much higher than did DHβE (Fig. 3, *middle* and *bottom*). Block by amantadine was notably voltage-dependent, with robust inhibition at more negative potentials, and almost none at membrane potentials more positive than −35 mV (Fig. 3, *bottom left*). In contrast, inhibition by quinine showed no voltage dependence (Fig. 3, *bottom left*). Voltage dependence of the amantadine block, as well as the reduced peak current amplitude with faster decay kinetics during coapplication with agonist (Fig. 3, *middle right*), suggests that amantadine acts as a channel blocker. Amantadine was fourfold less potent as a blocker of mutant (IC_{50} = 207 ± 30 μM) than wild-type (IC_{50} = 51 ± 10 μM) α4β2 AChRs (Fig. 3, *bottom right*). This reduction of potency in blocking mutant AChRs could be explained by reduced affinity of amantadine for its channel binding site caused by the S247F mutation in the ion channel lumen (Charnet et al., 1990; Leonard et al., 1991).

The S247F mutation in the M2 transmembrane domain of the α4β2 AChR decreases Ca^{2+} permeability of the channel

Currents through both mutant and wild-type α4β2 AChRs showed strong inward rectification characteristic of neuronal

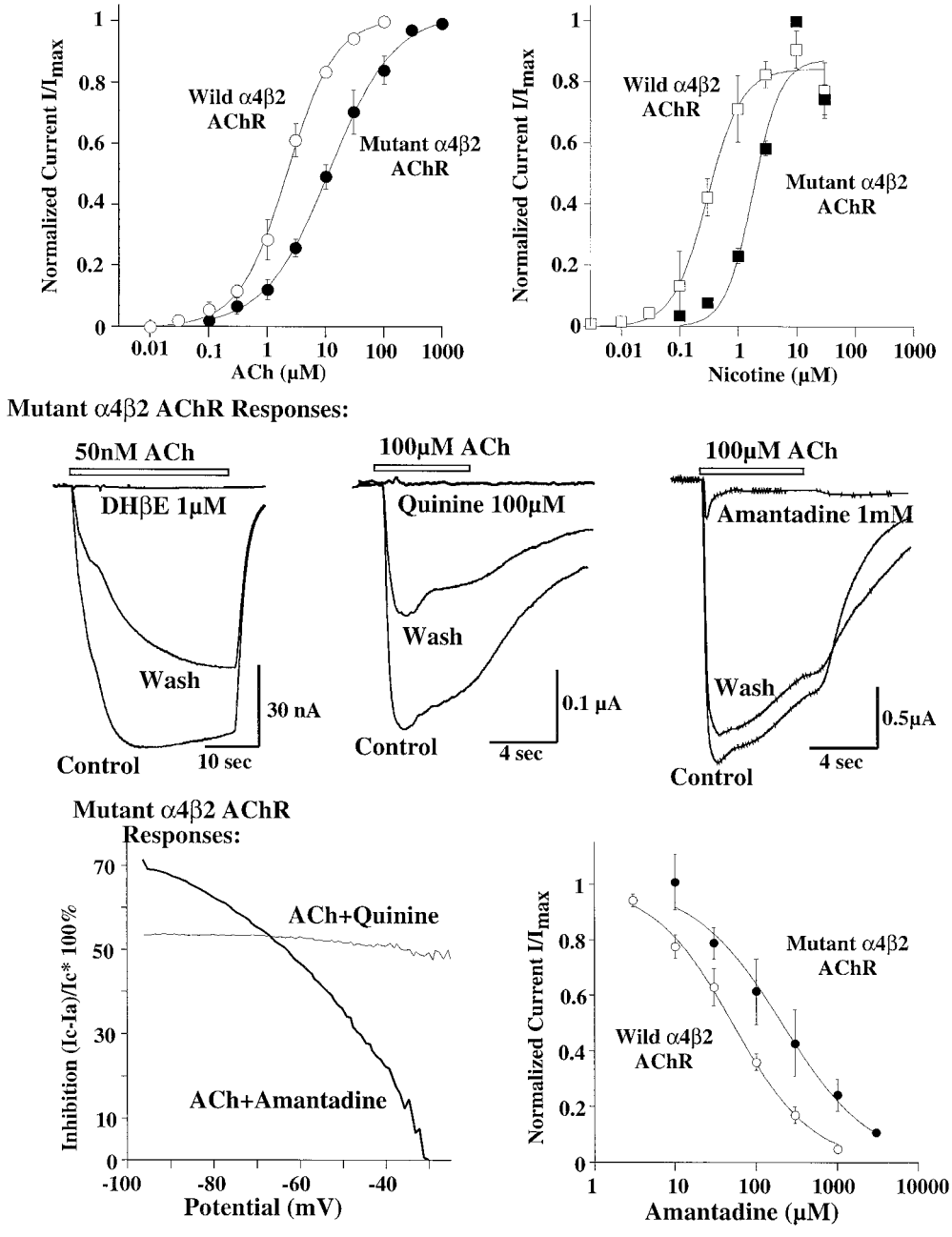

Figure 3. Comparison of pharmacological properties of human wild-type and mutant α4β2 AChRs. *Top*, Concentration/response curves for ACh and nicotine for wild-type and mutant α4β2 AChRs. *Middle,* Inhibition of mutant α4β2 AChR-mediated currents by DHβE, quinine, and amantadine. Equivalent inhibition of wild-type α4β2 AChRs was produced at these concentrations of DHβE and quinine. Control responses superimposed with responses induced by coapplication of ACh and antagonists, and responses induced after 5 min washout, are shown. *Bottom left,* Comparison of the voltage dependence of the inhibition of the mutant α4β2 AChRs by quinine (*thin line*) and amantadine (*thick line*) are shown. Voltage dependence is represented by plotting the amount of the inhibition $(I_c - I_a)/I_c \cdot 100\%$ against holding potential, where I_c is the current in the presence of the ACh (100 μM), and I_a is the current induced by coapplication of the ACh (100 μM) and quinine (10 μM) or amantadine (100 μM). Currents were measured by the application of 2 sec voltage ramps from −100 to +50 mV to the oocytes before and during application of the agonist or coapplication of the agonist and antagonist. Passive currents induced before application of the agonist were subtracted. *Bottom right*, Concentration/response curves built for amantadine inhibition of wild-type (*open circles*) and the mutant (*filled circles*) α4β2 AChRs. Data obtained from four to six oocytes held at −50 mV were normalized to the control responses induced by 100 μM ACh, averaged, and fit by using the Hill equation (EC_{50} and IC_{50} = values, and *n*H values are listed in the text).

AChRs, with outward currents at +50 mV being <5% of the current at −50 mV. The reversal potentials for both AChR subtypes were estimated by using ramp protocols applied during application of the agonist in Cl^--free media to prevent contamination with the endogenous Ca^{2+}-dependent Cl^- current. Currents mediated via wild-type AChRs reversed at −11.4 ± 1.4 mV (n = 15) under these conditions; for mutant AChRs the reversal occurred at −10.3 ± 1.2 mV (n = 11). Reversal of the wild-type

α4β2 AChR currents depended on the concentration of Ca^{2+} ions in the extracellular solution. When the concentration of Ca^{2+} was increased 10-fold from 1.8 to 18 mM, the reversal potential shifted in the positive direction by 4.4 ± 0.8 mV (Fig. 4, *top left* and *middle*). The same change of extracellular medium did not cause significant changes in the reversal potential of mutant α4β2 AChRs, although some tendency for a subtle shift to more negative potentials was observed (−0.7 ± 0.9 mV) (Fig. 4, *top right* and *middle*). Changes of the reversal potentials obtained by voltage ramps were virtually the same when current/voltage relationships were obtained from the peak current measurements from the oocytes voltage-clamped at different holding potentials (data not shown). From these data it appears that mutant α4β2 AChRs are significantly less permeable to Ca^{2+} than are wild-type AChRs.

Coexpression of the α5 subunit changed the permeability of mutant α4β2 AChRs. In 1.8 mM Ca^{2+} currents mediated via wild-type α4β2α5 AChRs reversed at −14.1 ± 0.7 mV ($n = 8$). Increasing the Ca^{2+} concentration to 18 mM shifted the reversal potential 7.0 ± 1.1 mV more positive. In 1.8 mM Ca^{2+} mutant α4β2α5 AChRs had a reversal potential at −5.3 ± 1.8 mV ($n = 7$). Increasing the Ca^{2+} concentration 10-fold caused a 6.8 ± 0.9 mV more positive shift of the reversal potential. Thus, incorporation of the α5 subunit into the mutant α4β2 AChR channel not only reversed but, in fact, somewhat enhanced the Ca^{2+} permeability as compared with the wild-type α4β2 AChR.

Differences in the Ca^{2+} permeability of wild-type and mutant α4β2 AChRs also were confirmed by an alternative method. When all cations but Ca^{2+} in the extracellular solution were replaced by an equiosmotic concentration of dextrose, wild-type α4β2 AChRs still conducted detectable inward current (Fig. 4, *bottom left*). The amplitude of this current was only 6 ± 1.0% of the current induced at the same membrane potential by the same concentration of agonist in the normal extracellular solution (ND-96). As expected, virtually no residual inward current was observed when similar replacement of the extracellular cations was performed on oocytes expressing mutant α4β2 AChRs (Fig. 4, *bottom middle*). These experiments confirmed that the S247F mutation of the α4 subunit dramatically decreased the ability of α4β2 AChRs to conduct Ca^{2+} ions. This impairment of the Ca^{2+} permeability of the mutant α4β2 AChR could be compensated for effectively by the introduction of the α5 subunit.

Comparison of single channel properties of wild-type and S247F α4β2 AChRs

Single channel currents were activated in outside-out patches for both wild-type and mutant α4β2 AChRs expressed in *Xenopus* oocytes (Figs. 5, 6). For both types of AChRs the sensitivity for channel activation was extremely high, so 50 nM ACh was used for steady-state recording. Recording at this concentration allowed for sufficient channel activity to be obtained for amplitude and kinetic analysis. Even at this low concentration, desensitization was evident, particularly for the mutant AChRs. For example, channel activity for the wild-type AChR was sustained for 3–5 min of continuous application of 50 nM ACh, whereas mutant AChR channels usually persisted for only 2–3 min before desensitizing. Moreover, channels could be reactivated by additional applications of agonist for the wild-type channels after a period of recovery, whereas the mutant channel activity was greatly diminished or completely inactivated.

Table 1. Single channel properties of native and αS247F mutant human α4β2 AChRs

AChR		Channel amplitudes (pA) (at −80 mV) (SE)	Mean channel open times (msec) (SE)	
			τ_1	τ_2
Mutant α4β2	γ_1	0.90	1.93	4.05
		(0.01)	(0.37)	(0.24)
Native α4β2	γ_1	1.35	3.65	23.4
		(0.06)	(0.51)	(4.76)
	γ_2	2.27	1.9	8.05
		(0.08)	(0.21)	(0.58)

Sensitivity to DHβE

The nicotinic character of single channel activity observed in outside-out patches from oocytes was confirmed by demonstrating sensitivity to DHβE. We found that coapplication of 1 μM DHβE could effectively antagonize the channels activated in outside-out patches by 50 nM ACh. Furthermore, the antagonism appeared to be competitive because, at the initial coapplication of ACh with DHβE, channel openings occurred that had the same amplitude and duration as the channels recorded in the absence of the antagonist. Additionally, when the number of channels in the patch was high, periodic openings of channels were observed that also resembled the channels in the absence of antagonist. The antagonism by DHβE was also readily reversible, because reapplication of ACh within 60 sec after removing DHβE resulted in a level of channel activity resembling the activity level seen before the application of the antagonist. In the case of the mutant, the relatively rapid inactivation of the channel never allowed for a dramatic recovery of channel activity after removal of the DHβE, but the level of channel activity observed on washout was significantly higher than that seen in the presence of the antagonist.

Channel amplitudes

At a holding potential of −80 mV, wild-type α4β2 AChRs had two amplitudes of 1.4 ± 0.1 and 2.3 ± 0.1 pA (assuming a 0 mV reversal potential yields chord conductance estimates of 17 and 28 pS). The proportions of channel openings to each of the conductance levels were 67.4 and 32.6%, respectively. Mutant α4β2 AChR channels, on the other hand, had a single conductance channel type with an amplitude of 0.90 ± 0.01 pA (or 11 pS with the zero reversal potential assumption). In some patches a few openings to a higher level were observed. Only in one such patch were enough openings observed to perform a reasonable fit to the amplitude distribution, with the amplitude being 1.5 pA.

Mean channel open times

In every patch for the wild-type AChRs, both conductances exhibited gating behavior that required two components to fit the channel open time distributions. The mean channel open times for the 17 pS channel were 3.65 ± 0.51 msec (51.1% of the distribution) and 23.4 ± 4.76 msec (48.8%), whereas for the 28 pS channel the open times were 1.90 ± 0.21 msec (67.8%) and 8.05 ± 0.58 msec (32.2%). For the mutant AChR, the predominant conductance observed required two components for the fitting of the open time distributions in one-half of the patches recorded, whereas the remaining patches could be fit by a single-component function. The time constants derived for the patches that required only a single component corresponded to one of the

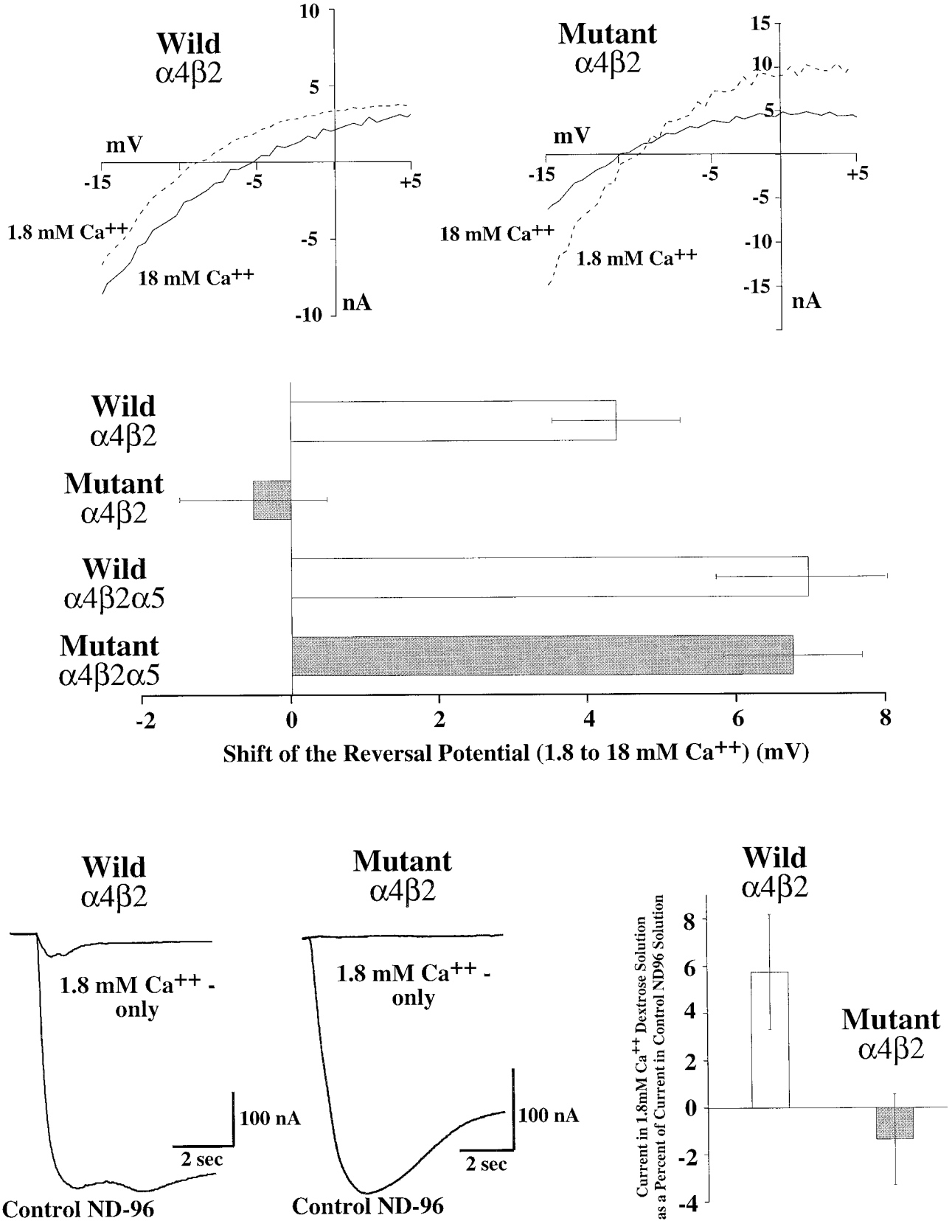

Figure 4. S247F mutation of the α4 subunit eliminates Ca^{2+} permeability of the α4β2 AChRs, which was restored by coexpression of α5 subunits. *Top*, Shift of the reversal potential of wild-type (*left*) and mutant (*right*) α4β2 AChRs induced by a 10-fold increase of Ca^{2+} concentration from 1.8 to 18 mM. Representative currents induced by the application of voltage ramps on oocytes perfused by 100 μM ACh with 1.8 mM (*dashed trace*) or 18 mM Ca^{2+} (*solid trace*) in the solution are plotted against membrane potential. Currents induced by the ramps in agonist-free solutions are subtracted. Recordings were performed in Cl^--free solutions on the oocytes preincubated in the Cl^--free media. *Middle*, Plot of the reversal potential (*Figure legend continues*)

components of the patches that required two component fits. The mean open times were 1.93 ± 0.37 msec (69.3%) and 4.05 ± 0.24 msec (30.7%).

DISCUSSION

In the present study we show that the S247F mutation in α4 subunits causes significant acceleration of desensitization and slows recovery from desensitization. Similar observations were made by Weiland et al. (1996) and Figl et al. (1997). Additionally, we characterized expression levels, functionality, pharmacological properties, Ca^{2+} permeability, channel conductance, and gating of the mutant in comparison with the wild-type α4β2 AChRs. All of these characteristics of the mutant α4β2 AChRs are important, both from the perspective of gaining a better understanding of the structure and function of AChRs and for better understanding possible mechanisms of seizures in ADNFLE patients.

The S247F mutation in human α4 subunits did not cause notable changes, at least in oocytes, in the expression efficiency of either α4β2 or α4β2α5 AChRs. Similar results were reported for rat S247F mutant α4β2 AChRs expressed in oocytes (Figl et al., 1997). These results suggest that changes in the amount of α4β2 AChRs are not responsible for pathological changes in ADNFLE.

Potentiation of the responses to agonist on successive exposures in the case of the αS247F mutant is an interesting phenomenon that may have implications for the pathological mechanisms of ADNFLE. This disease is characterized by seizures during light sleep (Scheffer et al., 1994, 1995). If α4β2 AChRs were associated with a generalized cholinergic activation mechanism regulating sleep and wakefulness, as has been suggested (Szymusiak, 1995; Everitt and Robbins, 1997), then mutant α4β2 AChRs might be susceptible to failure at the beginning of this transition, but after sustained activation during wakefulness (or sleep), the potentiated function of these mutant α4β2 AChRs into the normal range of function would prevent seizures during sustained wakefulness (or sleep).

The αS247F mutation had little effect on the EC_{50} of the ACh binding site ligands ACh or nicotine but did reduce the efficacy of the channel-blocking ligand amantadine. This is consistent with the putative location of this mutation being in the lumen of the channel near the gate at the cytoplasmic surface.

We observed virtually complete abolition of the permeability of Ca^{2+} ions through the mutant AChRs. The S247F mutation is located in the part of M2 thought to form the intermediate hydrophilic ring in the channel that contributes to cation selectivity (Imoto et al., 1988). Interestingly, mutant α4β2 AChRs regained Ca^{2+} permeability when the α5 subunit was incorporated in the channel. It has been proposed that α5 subunits in neuronal AChRs occupy a position around the cation channel corresponding to β1 subunits of muscle AChRs (i.e., α4β2α4β2α5) to account for the observations that α5 cannot form ACh binding sites or functional AChRs in combination with just β2 subunits but requires the presence of both α3 or α4 and β2 or β4 subunits (Ramirez-Latorre et al., 1996; Wang et al., 1996). Further structural studies of the α5 contribution into the nicotinic AChR channel are needed to understand the mechanism of this Ca^{2+} permeability compensation. This effect of the α5 subunits indicates that in the brains of ADNFLE patients it would be possible for α4β2α5 AChRs to function more nearly normally. Such a subtype would comprise only a small fraction of the total, because most brain α4 AChRs are not bound by mAbs to α5 (F. Wang, V. Gerzanich, and J. Lindstrom, unpublished data). Reduced Ca^{2+} permeability is a very important deficit in α4β2 AChR function because many of these AChRs may function presynaptically to facilitate transmitter release by increasing the presynaptic Ca^{2+} concentration.

The S247F mutation in the α4 subunit had a considerable impact on the single channel properties of the resulting AChRs. Whereas the AChRs containing wild-type α4 had two conductance states of the channels of approximately equal likelihood of appearance, the mutant AChRs seemed to prefer a lower conductance state of the channel. Considering the size and hydrophobicity of the phenyl group of phenylalanine as compared with the hydroxyl group of serine, it seems plausible that a conformation shift within the channel lumen necessary for transition into one of the conductance states is less likely in the mutant with a phenyl group. Because the preferred conductance state of the mutant channel has a conductance different from either of the wild-type channel conductances, serine 247 clearly contributes to the selectivity filter of the channel and not just to the regulation of conformational changes controlling the switch between the two conductance states. The fact that the main conductance state of the mutant was significantly smaller than either of the conductance states of the wild-type AChR seems reasonable, because the larger hydrophobic group of phenylalanine presumably would inhibit movement of ions through the channel, particularly large divalent cations like Ca^{2+}. The estimates of single channel conductances that we observed for wild-type human α4β2 ACHRs expressed in oocytes (17 and 28 pS) were in the same range as those for similarly expressed α4β2 AChRs from rats (12, 22, and 34 pS) or chickens (20 and 24 pS), considering differences in recording conditions (Charnet et al., 1990, 1992; Cooper et al., 1991; Ramirez-Latorre et al., 1996).

The channel open kinetics were also markedly dissimilar for the mutant as compared with the wild-type AChR. Both conductance types of the wild-type AChR demonstrated relatively long channel openings as compared with the mutant, particularly the lower conductance form of the wild-type channel, thus demonstrating the less energetically favored transition into the channel open state for the mutant form of the AChR. In addition to the brevity of the mutant AChR channel openings, channel desensitization for the mutant occurred much more rapidly than for the wild-type AChR during continuous application of 50 nM ACh, and the mutant was much less likely to recover activity after a period in control solution. Channel activity for the wild-type AChR usually could be observed for 3–5 min of continuous application and could be evoked by reapplication for periods of

←

shifts induced by a 10-fold increase of the extracellular Ca^{2+} concentration (from 1.8 to 18 mM) for wild-type (*open bars*) and mutant (*filled bars*) α4β2 and α4β2α5 AChRs. Averaged data obtained from 7 to 14 oocytes as described on the *top panel* represent mean value ± SE. *Bottom*, Currents conducted only by Ca^{2+} ions through wild-type and mutant α4β2 AChRs. *Left,* Currents induced in normal ND-96 media and an equiosmotic solution containing 1.8 mM Ca^{2+} as the only permanent ion were compared for both wild-type and mutant α4β2 AChRs. Currents were induced by 100 μM ACh in Cl^--free media. *Right*, Plot of the percentage of the inward current induced in the "Ca^{2+}-only" (1.8 mM) solution as compared with the current in the normal ND-96 solution for wild-type (*open bar*) and mutant (*shaded bar*) α4β2 AChRs. *Bar* in the negative direction for the mutant indicates that in some experiments currents were outward in the "Ca^{2+}-only" conditions. Data were obtained from seven oocytes preincubated in the Cl^--free media for each AChR; mean values and SE are plotted.

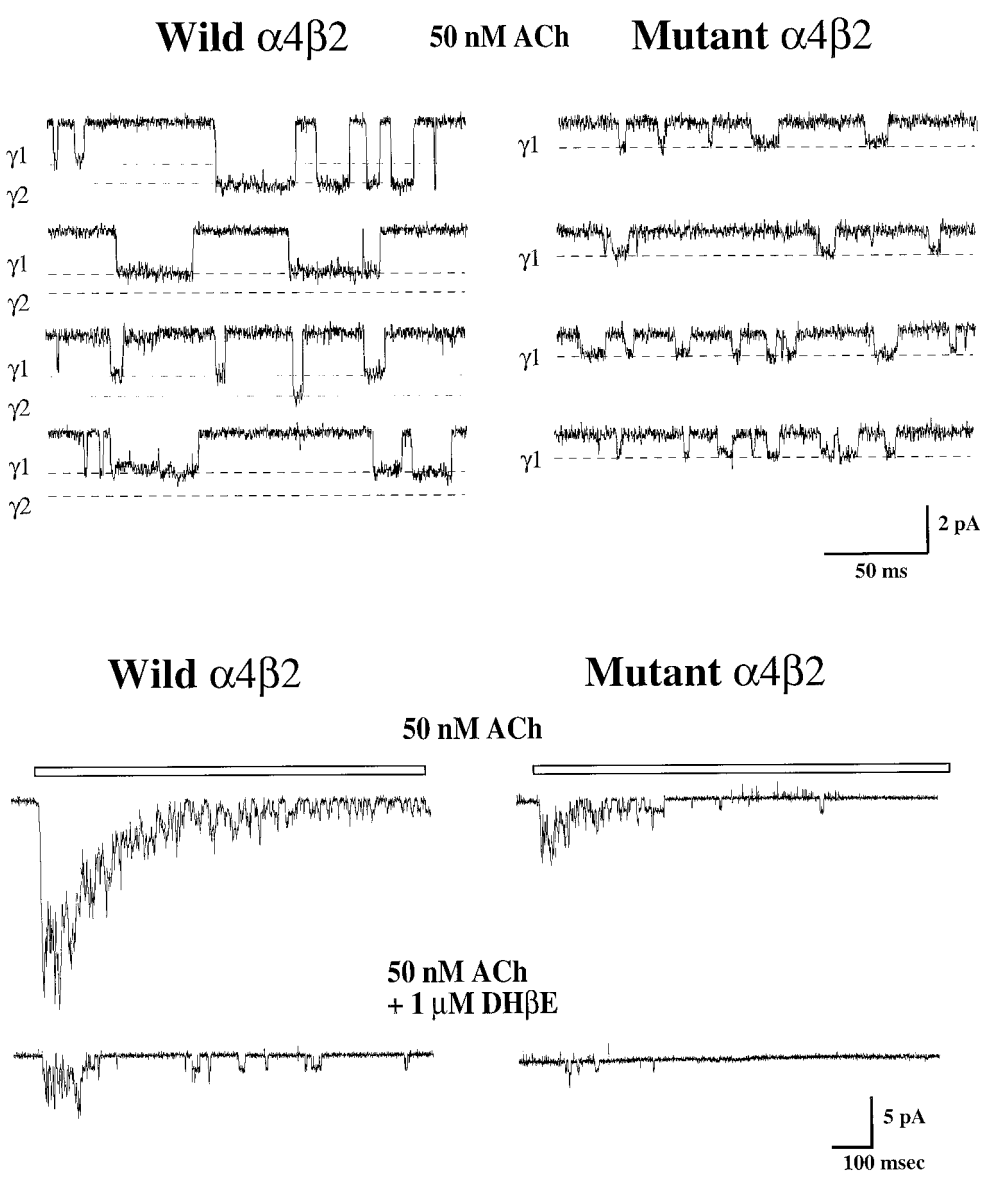

Figure 5. Single channel currents of the human wild-type and mutant $\alpha4\beta2$ AChRs. *Top*, Records are from outside-out patches taken from oocytes that were injected with either human $\alpha4\beta2$ or human αS247F mutant $\alpha4\beta2$ AChRs. Currents were recorded at −80 mV by steady-state application of 50 nM ACh, with the patch isolated in a continuously flowing stream of agonist diluted from stock into ND-96 solution. Channel activity was initiated by lateral displacement of the perfusion tube across the face of the recording electrode. Wild-type AChRs exhibited two conductance levels, as indicated by the *dashed lines*, whereas mutant AChRs exhibited predominantly a single conductance level. For display, records were sampled at 10 kHz and filtered at 2 kHz (eight-pole Bessel, −3 dB). *Bottom,* Both wild-type and mutant AChR single channel currents were blocked by 1 μM DHβE. Currents were activated originally by 50 nM ACh by rapid movement of the perfusion tube across the tip of the recording electrode. High levels of expression allowed robust inward currents to be observed because of massive simultaneous channel activations. After ~1 min of wash, agonist was reapplied along with 1 μM DHβE. The initial channel activity was significantly lower as compared with the level in the absence of antagonist. After the first 3–5 sec, the channel activity was essentially gone because of inhibition by DHβE. The inhibition was reversible within 60 sec (time for solution change).

15–20 min, whereas the mutant AChRs would inactivate during an initial 2–3 min period of continuous application. The net effect of the mutation on the single channel properties of $\alpha4\beta2$ AChRs is to decrease the capacity for the AChR to pass charge both during each gating of the channel and over a time-averaged period of continuous channel activation.

The net functional capacity of the S247F α4 mutants thus is reduced by four mechanisms that reduce the net flow of ions through activated AChRs: (1) Ca^{2+} permeability is lost, (2) desensitization is increased, (3) channel opening time is reduced, and (4) channel conductance is reduced. Two compensating mechanisms were identified: (1) incorporation of α5 subunits repairs the deficit in Ca^{2+} conductance, and (2) repeated activation can produce a conformation that is more activatable for at least 24 hr. However, the net effect of this mutation is to reduce AChR function. This effect is so potent that even in the heterozygous state the disease occurs. High doses of nicotinic agonists can produce seizures (Miner and Collins, 1988; Singer and Janz, 1990; Woolf et al., 1996), but loss of $\alpha4\beta2$ AChRs such as occurs in β2 knock-out mice (Picciotto et al., 1995) is not associated with the occurrence of seizures. Epilepsy is caused by excessive neuronal activation. How might a mutation that causes a net decrease in AChR function cause the excessive excitation characteristic of epilepsy? Neuronal AChRs are effective at promoting the release of many transmitters from synaptosomes (Role and Berg, 1996; Wonnacott, 1997). It seems likely that $\alpha4\beta2$ AChRs controlling the release of the inhibitory transmitters GABA or glycine either presynaptically or postsynaptically could be responsible for triggering seizures in ADNFLE. There are numerous studies describing nicotine-induced GABA release either from isolated synaptosomes or shown directly in electrophysiological studies (Lena et al., 1993; Kayadjanian et al., 1994; McMahon et al., 1994; Role and Berg, 1996; Wonnacott, 1997). Nicotine was shown to cause or potentiate release of other inhibitory neurotransmitters, i.e., dopamine, serotonin, adenosine, and ACh (Brudzynski et al., 1991; Cruickshank et al., 1994; Role and Berg, 1996; Wilkie et al., 1996; Yang et al., 1996; Wonnacott, 1997). ADNFLE can be treated effectively by the sodium channel blocker carbamazepine (Scheffer et al., 1994). This leaves the question open of which neurotransmitters besides ACh are involved in the pathology.

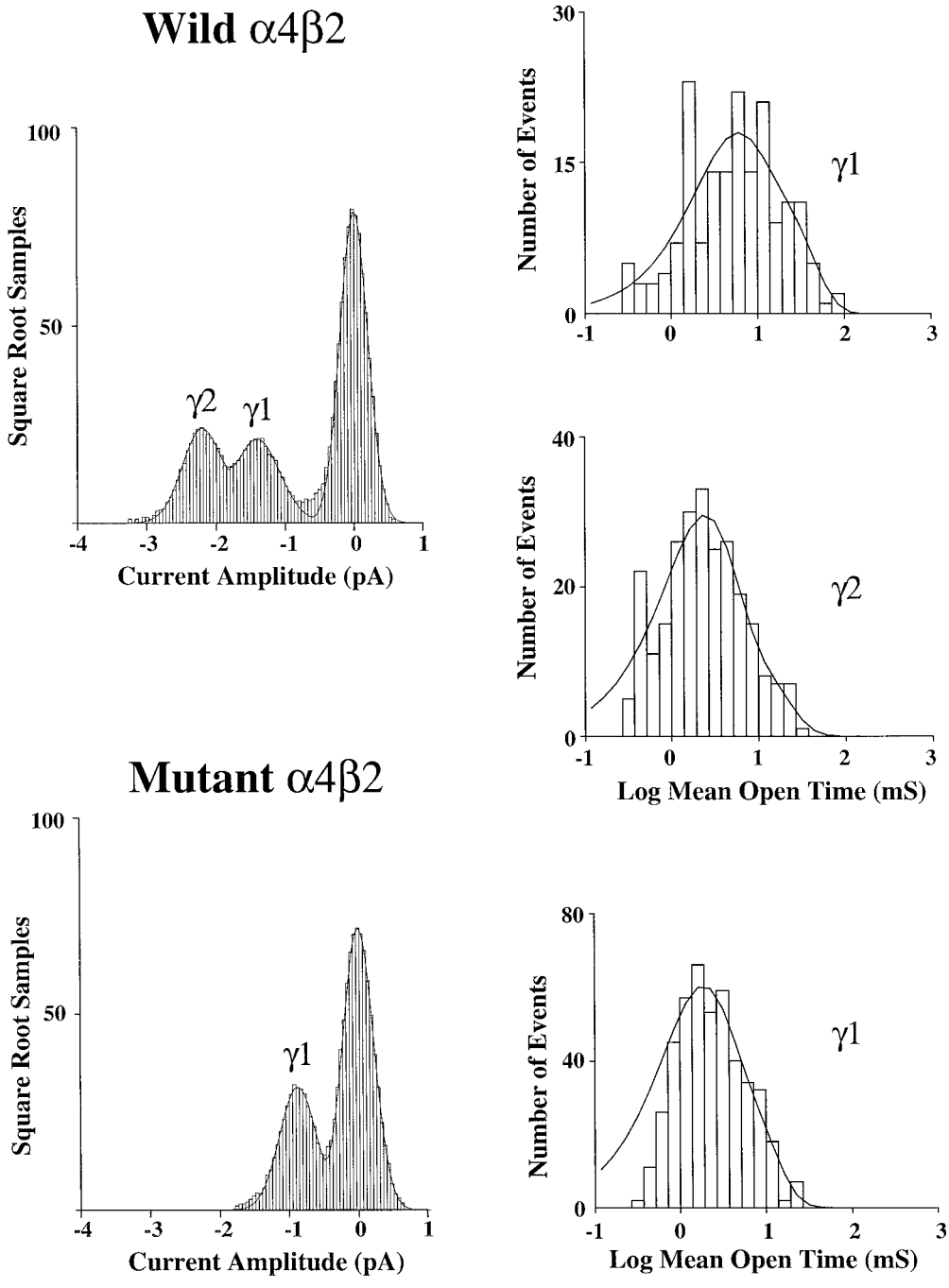

Figure 6. Single channel properties of wild-type and mutant α4β2 AChRs. *Left,* Representative unitary conductance histograms. All-point amplitude histograms were generated from sections of data files that did not contain simultaneous channel openings. The data are presented as the square root of samples to emphasize the channel open amplitudes. Fitting of the histograms was done by a Levenburg–Marquardt least-squares algorithm of either three (wild-type) or two (mutant) gaussian components. *Right,* Channel open time histograms were generated from events list files. In all cases, the fits shown represent a Simplex maximum likelihood estimate of a two-component exponential function. The mean values for the time constants of the fits can be found in Table 1.

Occurrence of ADNFLE seizures in a strict relationship to the sleep–wake cycle indicates a possible involvement of cholinergic ascending brain stem systems (Meierkord, 1994; Szymusiak, 1995; Everitt and Robbins, 1997). Further physiological studies are needed to clarify the mechanisms of involvement of mutant α4 AChRs in the ADNFLE.

Recently, five mutations in the M2 transmembrane domain of the muscle nicotinic AChRs were identified as responsible for congenital myasthenic syndromes (CMS) (Ohno et al., 1995; Engel et al., 1996). In addition, mutations causing CMS also have been found in other parts of α1, β1, δ, and ϵ subunits (Engel et al., 1993, 1996; Gomez and Gammack, 1995; Ohno et al., 1995, 1996; Sine et al., 1995; Gomez et al., 1996). A total of >60 muscle AChR mutants has been found (A. Engel, personal communica-

tion). Properties of the recombinant mutated AChRs were compared with the properties of native AChRs from the intercostal muscle tissue obtained by biopsy from patients. Because the functional roles of $\alpha4\beta2$ AChRs are less well known and the tissue is inaccessible, such elegant analysis will not soon be possible on neuronal AChRs. However, the recent groundswell in discovery of mutations in muscle AChRs suggests that there also may be many such mutations in neuronal AChRs waiting to be discovered.

REFERENCES

Akabas M, Kaufmann C, Archdeacon P, Karlin A (1994) Identification of acetylcholine receptor channel-lining residues in the entire M2 segment of the α subunit. Neuron 13:919–927.

Anand R, Conroy WG, Schoepfer R, Whiting P, Lindstrom J (1991) Neuronal nicotinic acetylcholine receptors expressed in *Xenopus* oocytes have a pentameric quaternary structure. J Biol Chem 266:11192–11198.

Anand R, Bason L, Saedi MS, Gerzanich V, Peng X, Lindstrom J (1993) Reporter epitopes: a novel approach to examine transmembrane topology of integral membrane proteins applied to the α1 subunit of the nicotinic acetylcholine receptor. Biochemistry 32:9975–9984.

Bertrand D, Galzi JL, Devillers-Thiery A, Bertrand S, Changeux JP (1993) Mutations at two distinct sites within the channel domain M2 alter calcium permeability of neuronal α7 nicotinic receptor. Proc Natl Acad Sci USA 90:6971–6975.

Brudzynski SM, McLachlan RS, Girvin JP (1991) Involvement of M1 and M2 muscarinic receptors of the basal forebrain in cholinergically mediated changes in the rat locomotion. Prog Neuropsychopharmacol Biol Psychiatry15:279–284.

Charnet P, Labarca C, Leonard RJ, Vogelaar NJ, Czyzyk L, Gouin A, Davidson N, Lester HA (1990) An open-channel blocker interacts with adjacent turns of α-helices in the nicotinic acetylcholine receptor. Neuron 4:87–95.

Charnet P, Labarca C, Cohen B, Davidson N, Lester H, Pilar P (1992) Pharmacological and kinetic properties of $\alpha4\beta2$ neuronal nicotinic acetylcholine receptors expressed in *Xenopus* oocytes. J Physiol (Lond) 450:375–394.

Cooper E, Couturier S, Ballivet M (1991) Pentameric structure and subunit stoichiometry of a neuronal nicotinic acetylcholine receptor. Nature 350:235–238.

Cruickshank JW, Brudzynski SM, McLachlan RS (1994) Involvement of M1 muscarinic receptors in the initiation of cholinergically induced epileptic seizures in the rat brain. Brain Res 643:125–129.

Engel AG, Uchitel OD, Walls TJ, Nagel A, Harper CM, Bodensteiner J (1993) Newly recognized congenital myasthenic syndrome associated with high conductance and fast closure of the acetylcholine receptor channel. Ann Neurol 34:38–47.

Engel AG, Ohno K, Milone M, Wang HL, Nakano S, Bouzat C, Pruitt JN, Hutchinson DO, Brengman JM, Bren N, Sieb JP, Sine SM (1996) New mutations in acetylcholine receptor subunit genes reveal heterogeneity in the slow-channel congenital myasthenic syndrome. Hum Mol Genet 5:1217–1227.

Everitt B, Robbins T (1997) Central cholinergic systems and cognition. Annu Rev Psychol 48:649–684.

Figl A, Viseshakul N, Forsayeth J, Cohen BN (1997) A mutation associated with epilepsy enhances desensitization of the $\alpha4\beta2$ neuronal nicotinic receptor. Biophys J 72:A150.

Filatov GN, White MM (1995) The role of conserved leucines in the M2 domain of the acetylcholine receptor in channel gating. Mol Pharmacol 48:379–384.

Forman SA, Yellen G, Thiele EA (1996) Alternative mechanism for pathogenesis of an inherited epilepsy by a nicotinic AChR mutation [letter]. Nat Genet 13:396–397.

Francis M, Papke R (1996) Muscle-type nicotinic acetylcholine receptor delta subunit determines sensitivity to noncompetitive inhibitors, while the γ subunit regulates divalent permeability. Neuropharmacology 35:1547–1556.

Gerzanich V, Anand R, Lindstrom J (1994) Homomers of α8 and α7 subunits of nicotinic receptors exhibit similar channel but contrasting binding site properties. Mol Pharmacol 45:212–220.

Gomez CM, Gammack JT (1995) A leucine-to-phenylalanine substitution in the acetylcholine receptor ion channel in a family with the slow-channel syndrome. Neurology 45:982–985.

Gomez CM, Maselli R, Gammack J, Lasalde J, Tamamizu S, Cornblath DR, Lehar M, McNamee M, Kuncl RW (1996) A β-subunit mutation in the acetylcholine receptor channel gate causes severe slow-channel syndrome. Ann Neurol 39:712–723.

Gopalakrishnan M, Monteggia L, Anderson D, Molinari E, Piattoni-Kaplan M, Donnelly-Roberts D, Arneric S, Sullivan J (1996) Stable expression, pharmacological properties, and regulation of the human neuronal nicotinic acetylcholine $\alpha4\beta2$ receptor. J Pharmacol Exp Ther 276:289–297.

Harvey SC, Maddox FN, Luetje CW (1996) Multiple determinants of dihydro-β-erythroidine sensitivity on rat neuronal nicotinic receptor α subunits. J Neurochem 67:1953–1959.

Imoto K, Busch C, Sakmann B, Mishina M, Konno T, Nakai J, Bujo H, Mori Y, Fukuda K, Numa S (1988) Rings of negatively charged amino acids determine the acetylcholine receptor channel conductance. Nature 335:645–648.

Kayadjanian N, Retaux S, Menetrey A, Besson MJ (1994) Stimulation by nicotine of the spontaneous release of [^{3}H]gamma-aminobutyric acid in the substantia nigra and in the globus pallidus of the rat. Brain Res 649:129–135.

Lena C, Changeux JP, Mulle C (1993) Evidence for "preterminal" nicotinic receptors on GABAergic axons in the rat interpeduncular nucleus. J Neurosci 13:2680–2688.

Leonard JP, Kelso SR (1990) Apparent desensitization of NMDA responses in *Xenopus* oocytes involves calcium-dependent chloride current. Neuron 4:53–60.

Leonard RJ, Charnet P, Labarca C, Vogelaar NJ, Czyzyk L, Gouin A, Davidson N, Lester HA (1991) Reverse pharmacology of the nicotinic acetylcholine receptor. Mapping the local anesthetic binding site. Ann NY Acad Sci 625:588–599.

Lindstrom J, Anand R, Peng X, Gerzanich V, Wang F, Li Y (1995) Neuronal nicotinic receptor subtypes. Ann NY Acad Sci 757:100–116.

Matsubayashi H, Swanson K, Albuquerque E (1997) Amantadine inhibits nicotinic acetylcholine receptor function in hippocampal neurons. J Pharmacol Exp Ther 281:834–844.

McMahon LL, Yoon KW, Chiappinelli VA (1994) Nicotinic receptor activation facilitates GABAergic neurotransmission in the avian lateral spiriform nucleus. Neuroscience 59:689–698.

Meierkord H (1994) Epilepsy and sleep. Curr Opin Neurol 7:107–112.

Melton D, Kreig P, Rebagliati M, Maniatis T, Zinn K, Green M (1984) Efficient *in vitro* synthesis of biologically active RNA and RNA hybridization probes from plasmids containing a bacteriophage SP6 promoter. Nucleic Acids Res 12:7035–7056.

Miner LL, Collins AC (1988) The effect of chronic nicotine treatment on nicotine-induced seizures. Psychopharmacology 95:52–55.

Ohno K, Hutchinson DO, Milone M, Brengman JM, Bouzat C, Sine SM, Engel AG (1995) Congenital myasthenic syndrome caused by prolonged acetylcholine receptor channel openings due to a mutation in the M2 domain of the ε subunit. Proc Natl Acad Sci USA 92:758–762.

Ohno K, Wang HL, Milone M, Bren N, Brengman JM, Nakano S, Quiram P, Pruitt JN, Sine SM, Engel AG (1996) Congenital myasthenic syndrome caused by decreased agonist binding affinity due to a mutation in the acetylcholine receptor epsilon subunit. Neuron 17:157–170.

Peng X, Gerzanich V, Anand R, Whiting P, Lindstrom J (1994) Nicotine-induced increase in neuronal nicotinic receptors results from a decrease in the rate of receptor turnover. Mol Pharmacol 46:523–530.

Phillips HA, Scheffer IE, Berkovic SF, Hollway GE, Sutherland GR, Mulley JC (1995) Localization of a gene for autosomal dominant nocturnal frontal lobe epilepsy to chromosome 20q 13.2. Nat Genet 10:117–118.

Picciotto M, Zoli M, Lena C, Bessis A, Lallemand Y, Lenovere N, Vincent P, Rich E, Brulet P, Changeux J-P (1995) Abnormal avoidance learning in mice lacking functional high-affinity nicotine receptor in the brain. Nature 374:65–67.

Ramirez-Latorre J, Yu CR, Qu X, Perin F, Karlin A, Role L (1996) Functional contributions of α5 subunit to neuronal acetylcholine receptor channels. Nature 380:347–351.

Riedel WJ, Jolles J (1996) Cognition enhancers in age-related cognitive decline. Drugs Aging 8:245–274.

Role LW, Berg DK (1996) Nicotinic receptors in the development and modulation of CNS synapses. Neuron 16:1077–1085.

Scheffer IE, Bhatia KP, Lopes-Cendes I, Fish DR, Marsden CD, Andermann F, Andermann E, Desbiens R, Cendes F, Manson JI, Berkovic S

(1994) Autosomal dominant frontal epilepsy misdiagnosed as sleep disorder. Lancet 343:515–517.

Scheffer IE, Bhatia KP, Lopes-Cendes I, Fish DR, Marsden CD, Andermann E, Andermann F, Desbiens R, Keene D, Cendes F, Manson J, Constantinou J, McIntosh A, Berkovic S (1995) Autosomal dominant nocturnal frontal lobe epilepsy: a distinctive clinical disorder. Brain 118:61–73.

Sigworth F, Sine S (1987) Data transformation for improved display and fitting of single channel dwell time histograms. Biophys J 52:1047–1054.

Sine SM, Ohno K, Bouzat C, Auerbach A, Milone M, Pruitt JN, Engel AG (1995) Mutation of the acetylcholine receptor α subunit causes a slow-channel myasthenic syndrome by enhancing agonist binding affinity. Neuron 15:229–239.

Singer J, Janz T (1990) Apnea and seizures caused by nicotine ingestion. Pediatr Emerg Care 6:135–137.

Steinlein OK, Mulley JC, Propping P, Wallace RH, Phillips HA, Sutherland GR, Scheffer IE, Berkovic SF (1995) A missense mutation in the neuronal nicotinic acetylcholine receptor α4 subunit is associated with autosomal dominant nocturnal frontal lobe epilepsy. Nat Genet 11:201–203.

Steinlein O, Magnusson A, Stoodt J, Bertrand S, Weiland S, Berkovic S, Nakken K, Propping P, Bertrand D (1997) An insertion of the CHRNA4 gene in a family with autosomal dominant nocturnal lobe epilepsy. Hum Mol Genet 6:943–947.

Szymusiak R (1995) Magnocellular nuclei of the basal forebrain: substrates of sleep and arousal regulation. Sleep 18:478–500.

Vernino S, Amador M, Luetje CW, Patrick J, Dani JA (1992) Calcium modulation and high calcium permeability of neuronal nicotinic acetylcholine receptors. Neuron 8:127–134.

Vidal C, Changeux JP (1996) Neuronal nicotinic acetylcholine receptors in the brain. News Physiol Sci 11:202–208.

Wada E, Wada K, Boulter J, Deneris E, Heinemann S, Patrick J, Swanson LW (1989) Distribution of α2, α3, α4, and β2 neuronal nicotinic receptor subunit mRNAs in the central nervous system: a hybridization histochemical study in the rat. J Comp Neurol 284:314–335.

Wang F, Gerzanich V, Wells GB, Anand R, Peng X, Keyser K, Lindstrom J (1996) Assembly of human neuronal nicotinic receptor α5 subunits with α3, β2, and β4 subunits. J Biol Chem 271:17656–17665.

Weiland S, Witzemann V, Villarroel A, Propping P, Steinlein O (1996) An amino acid exchange in the second transmembrane segment of a neuronal nicotinic receptor causes partial epilepsy by altering its desensitization kinetics. FEBS Lett 398:91–96.

Whiting PJ, Lindstrom JM (1988) Characterization of bovine and human neuronal nicotinic acetylcholine receptors using monoclonal antibodies. J Neurosci 8:3395–3404.

Wilkie GI, Hutson P, Sullivan JP, Wonnacott S (1996) Pharmacological characterization of a nicotinic autoreceptor in rat hippocampal synaptosomes. Neurochem Res 21:1141–1148.

Wonnacott S (1997) Presynaptic nicotinic ACh receptors. Trends Neurosci 20:92–98.

Woolf A, Burkhart K, Caraccio T, Litovitz T (1996) Self-poisoning among adults using multiple transdermal nicotine patches. J Toxicol Clin Toxicol 34:691–698.

Yang X, Criswell HE, Breese GR (1996) Nicotine-induced inhibition in medial septum involves activation of presynaptic nicotinic cholinergic receptors on gamma-aminobutyric acid-containing neurons. J Pharmacol Exp Ther 276:482–489.

Zhang M, Wang Y, Vyas D, Neuman R, Bieger D (1993) Nicotinic cholinoceptor-mediated excitatory postsynaptic potentials in rat nucleus ambiguus. Exp Brain Res 96:83–88.